ETH zürich

Assessing Groundwater Abstraction for Irrigation Based on Electricity Consumption in Guantao County, China

Institute of Environmental Engineering
at ETH Zürich

Master Thesis

presented by

Andreas Hagmann

Zürich, 13.02.2017

Supervisors: Prof. Dr. W. Kinzelbach
Dr. L. Wang

Abstract

In the North China Plain, the over-pumping of groundwater during the last decades lead to a drastic decline in the water table. In combination with an expected increase in the occurrences of drought periods under climate change, there is need for a more sustainable groundwater management. The electric energy consumption for irrigation represents a cost-efficient tool to monitor and even restrict groundwater abstraction. However, a conversion factor is necessary to link the two. A first approach applied to compute said factor on a regional scale taking influential factors into account was based on a publication by the U.S. Geological Survey. A second, more specific one has been developed within the scope of the thesis at hand. The data basis was provided by the records from two sets of pumping tests in 2016, time series of the static depth to the water table, and a survey conducted in 2011 listing certain characteristic of each well in the study region. Analyses were carried out using MATLAB®. It could be shown that, on a regional scale, the conversion factor does not vary greatly throughout a period of four years (between 0.9 and 2.1 %). The results also suggest that a regional conversion factor determined on the basis of measurements at one location may be representative for the whole study region. This does, nevertheless, not hold for one individual well. If fairness among the farmers is one priority, separate conversion factors for different wells are of importance. The code may also be used to define a timeframe during which an experimentally determined conversion factor would likely represent the longterm average. Further development of the approach aims at incorporating continuous losses and improving the results, primarily by enhancing the data basis.

Contents

List of Tables

List of Figures

1 Introduction

In 2014, Wolfgang Kinzelbach initiated a Sino-Swiss research project entitled "Rehabilitation and management strategy for over-pumped aquifers under a changing climate". It tackles the challenges posed by groundwater overexploitation in arid regions in the context of climate change and focuses on two pilot regions, the Heihe River Basin in the province of Gansu and the region of Handan in the North China Plain. Agricultural production relies on intensive irrigation in the prevalent climate. Groundwater is the primary source therefor and has hence been overexploited in the past decades. In the future, the occurrences of drought periods are expected to increase calling for an improved water resources management. Aquifers are particularly suited to provide insurance against climate extremes as they are able to store water over years. Therefore, the goal of the project is to implement a real-time groundwater monitoring, modelling and controlling system in an effort to preserve or restore an aquifer's capability to mitigate droughts. It can eventually be used to determine abstraction quota by combining all observation data on groundwater levels, pumping rates, surface water imports and meteorology.
The thesis at hand focuses on the region of Handan. In order to restrict the water volume pumped at each well, a measuring device would have to be installed. However, a monitoring system consisting of flow meters is very expensive to install and maintain, and would have to be protected against tampering. Since the use of electrical pumps is common in the area and farmers have to pay for electricity, the consumption is already being determined for each well. Hence it also represents a cost-efficient way to monitor groundwater abstraction. At the same time, the latter can be reduced by restricting the electric energy consumption. In the final stage of the project, an IC card shall be necessary to bring the pumps into service. It carries the quota determined by the monitoring and modelling system. A conversion factor α [kWh/m^3], however, is needed. During two sets of pumping tests in 2016, α had been determined for a total of 127 individual wells by measuring the volumetric flow rate Q and determining the total power consumed N:

$$\alpha = \frac{N}{Q} \tag{1.1}$$

These data provide the basis for the analyses carried out within the scope of this thesis. The main objective was to determine the conversion factor under consideration of influential factors including the type of the pump, its age and the depth to the groundwater table. Two main approaches were chosen, a multiple linear regression as well as calculations based on the digitalisation of characteristic curves. This allowed the computation of a regional value of α. The total volume pumped could then be calculated by means of estimates of electric energy consumption for irrigation. Using three time series of the depth to the static water table obtained in three different locations,

an assessment of how annual and seasonal (irrigation seasons) values compare among themselves and among the three locations was made possible. Furthermore, a sensitivity analysis could be performed regarding the drawdown added to the static depth. MATLAB® was the primary analysis tool.
The structure of the document follows the subsequent pattern: The next two sections provide a general overview on the study region and its hydrogeological setting. The second chapter starts with theoretical remarks regarding pumps and pipe flow. It then addresses the two approaches to compute α, the data used and the main MATLAB script in a more detailed fashion. In the succeeding chapter, the results are presented in separate sections for each approach. The fourth chapter discusses the results and draws conclusions.

1.1 Study Region

The North China Plain (NCP) is a region of high social, economical and agricultural importance. It is a vital industrial region and, in addition, produces approx. 25 % of China's total grain yield. During summer, primarily maize grows on the fields and winter wheat between autumn and spring (Liu et al., 2001; Garduño and Foster, 2010).
The pilot site in the region of Handan itself is Guantao County lying in the south of Hebei Province (fig. 1.1). It covers an area of 456 km^2, whereof 32,000 ha are irrigated arable land, and has a population of 350,000. The prevalent continental monsoon climate leads to cold and dry winters, and hot and rainy summers with variable rainfall (Xu et al., 2005). Until the 1960s, the main water resource was the moderate rainfall (approx. 530 mm/a) as well as surface water (Liu et al., 2001; Garduño and Foster, 2010). The irrigation canals carried water from local rivers which were regulated by reservoirs in the upstream hills. Thereupon, to support the urban and industrial expansion of the major cities, these flows were transferred to those urban areas (Garduño and Foster, 2010). Since the annual rainfall, however, cannot cover the water consumption of summer maize (360 mm/a) and winter wheat (450 mm/a), the fields in the North China Plain have to be irrigated to maintain high levels of crop production. The situation is exacerbated by the fact that less rain falls during the winter whereas those crops require more water to prosper (Liu et al., 2001). As a consequence thereof, the farmers drilled wells to fill the gap between water demand and supply (Garduño and Foster, 2010). The expansion of cities, industries and irrigated area lead to groundwater overexploitation in the province of Hebei (Liu et al., 2001).

1.2 Hydrogeological Setting

A thick sequence of Quaternary sediments underlie Guantao County. The first 50 - 80 m of deposits form an unconfined shallow silt-sand aquifer containing freshwater (TDS $<$ 2,000 mg/l). Its saturated thickness typically reaches values of 20 - 30 m, however, it can be close to 0 m locally. Below lies a leaky aquitard carrying brackish groundwater which contains elevated concentrations of total dissolved solids (5,000 - 10,000 mg/l). Thereupon follows a deeper semi-confined sandy aquifer from 120 - 200 m below ground onwards (Garduño and Foster, 2010). The shallow aquifer

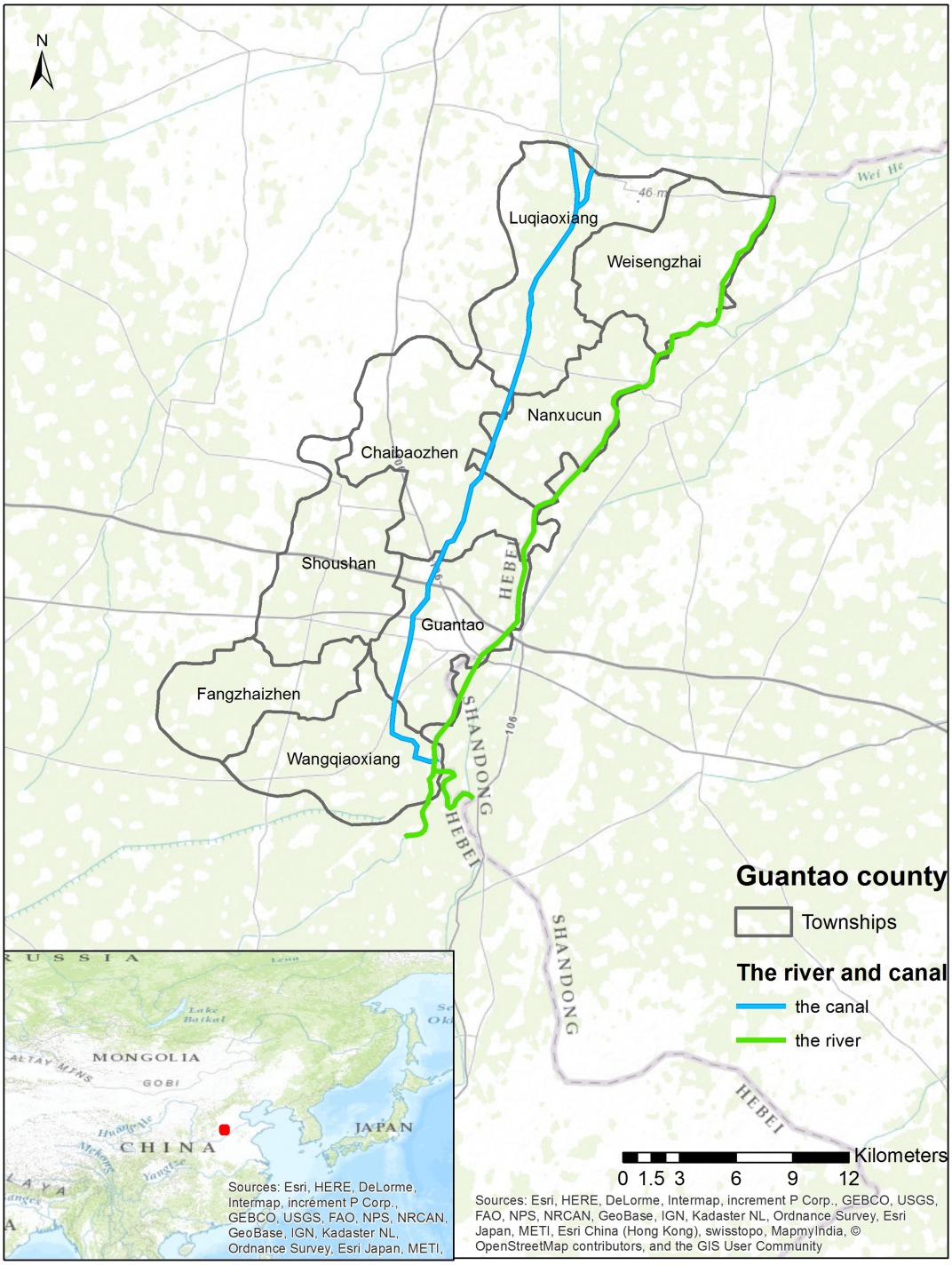

Figure 1.1: Small image: Lay of Guantao County within China. Large image: Borders of the county and its eight districts. The blue line represents the Weixi Canal whereas the green one shows the course of the Weiyun River.

underlies 60 - 70 % of the county's area whereas the deeper one as well as the aquitard are present throughout (Foster and Garduño, 2004).
Jia (2011) states that, until the 1960s, the two aquifers mentioned above were characterised by precipitation-infiltration recharge and evaporation-runoff drainage. The fluctuations in groundwater levels were in phase with precipitation. Since the large-scale groundwater exploitation started in the 1970s, the very same thing replaced evaporation-runoff drainage. Excess rainfall still forms the main component of recharge in Guantao County together with limited seepage from the river and the canal. Impoundment and infiltration of the summer runoff between June and September through field dykes, seepage from artificial ponds and spate irrigation further enhance it (Garduño and Foster, 2010). Figure 1.2 shows the drawdown of the static water table in both the shallow and the deep aquifer. Levels in the upper one of the two (solid line) decreased from 3.58 m in 1973 to 23 m in 2016 corresponding to mean decline of 0.46 m/a. Since 1999, however, only a slight downwards trend has been observed. The semi-confined deep aquifer exhibited artesian overflowing groundwater before the exploitation started (Garduño and Foster, 2010). Levels have dropped from 3.41 m (1973) to 69.5 m (2015), corresponding to an average decline of 1.57 m/a. Here, the downwards trend has still been strong during recent years. Furthermore, the over-pumping may lead to groundwater salinisation due to the presence of the leaky aquitard. In the shallow aquifer, heavy abstraction could cause up-coning of the brackish water formation. In the underlying deep aquifer, downward movement of brackish water induced by water abstraction poses a threat. The latter has already been monitored at average rates of 0.5 -1.5 m/a adding up to a total of 18 m from 1990 until 2010 (Foster and Garduño, 2004; Garduño and Foster, 2010).

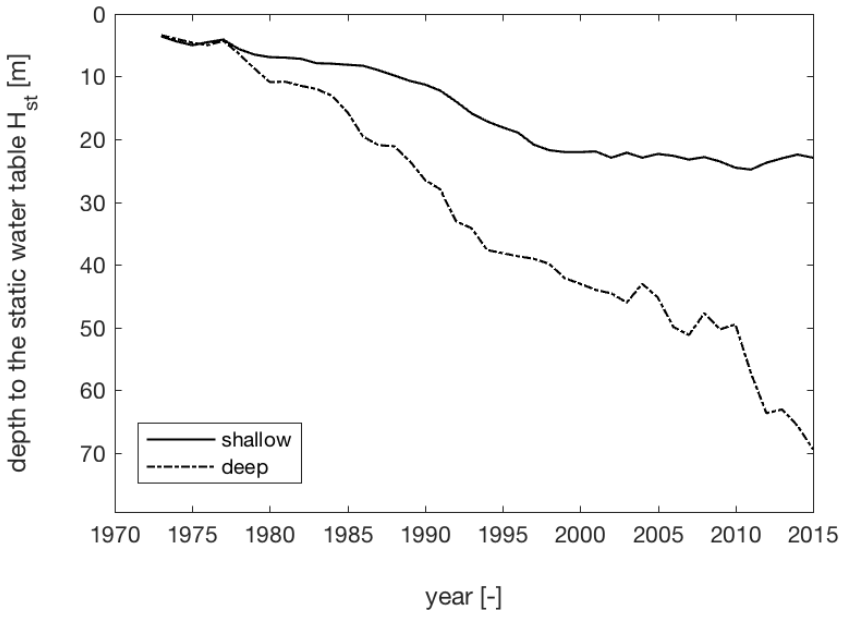

Figure 1.2: Drawdown of the static water table in the shallow (solid) and deep (dash-dot) aquifer in Guantao County between 1973 and 2015. A mean annual value was computed by averaging two measurements carried out in May and September, respectively. (Data: table A.2 in the appendix).

2 Materials and Methods

2.1 Theoretical Background

2.1.1 Pumps

Pumps supply water with mechanical energy. The electrical power needed to provide a flow rate Q with a lift H is given by (Gujer, 2007):

$$N_m = \frac{Q \cdot H \cdot \rho_w \cdot g}{\eta_p \cdot \eta_{motor}} \tag{2.1}$$

N_m	required power to the motor [W]
Q	volumetric flow rate [m^3/s]
H	discharge head [m]
ρ_w	density of water [kg/m^3]
g	acceleration due to gravity [m/s^2]
η_p	pump efficiency [-]
η_{motor}	motor efficiency [-]

Pump manufacturers provide information on their products e.g. in the form of a characteristic curve sheet (cf. fig. 2.1). These graphs usually show H, N_s or η_p as a function of Q. The shaft power N_s equals N_m multiplied by η_{motor}. Therefore, if an N_s is read from the figure for a given flow rate, the pump efficiency is already taken into account. The motor efficiency can be read from a table in the data sheet and may vary with the rated power of the pump.

2.1.2 Pipe Flow

One variable influencing the continuous friction losses in pipes is the dimensionless friction factor λ. The Prandtl-Colebrook equation allows for its computation (Gujer, 2007):

$$\frac{1}{\sqrt{\lambda}} = -2 \cdot \log_{10}\left(\frac{2.52}{Re \cdot \sqrt{\lambda}} + \frac{k/D}{3.71}\right) \tag{2.2}$$

λ	friction factor [-]
Re	Reynolds number [-]
k	equivalent sand roughness [m]
D	diameter of the pipe [m]

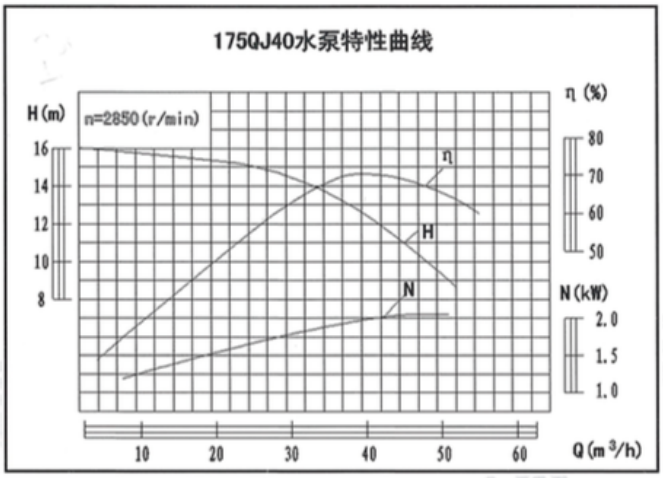

Figure 2.1: Example of characteristic curves showing the Q-H, Q-N_s and Q-η_p relationship for an engine speed of 2850 r/min. In xxxQJyy (see graph title), xxx stands for the device diameter and yy for the volumetric flow rate. (Taken from Hebei Linquan Pump Co. Ltd. (2015)).

Note that equation 2.2 can only be solved implicitly. A function could be obtained from the MathWorks File Exchange which solves for λ in an iterative fashion. The initial guess is based on the Haaland equation (equ. A.1 in the appendix). A short MATLAB script was then written which feeds the necessary inputs (Re, k and D) into said function. Values for the equivalent sand roughness k were taken from Bollrich (2013) and amounted to 0.003 mm for plastic pipes and 0.1 mm for metal ones, respectively. The former was also assigned to wells where the material of the pipe was not defined. Refer to the appendix for the computation of Re (equations A.2 and A.3).

2.2 USGS Method

The first approach taken was based on a paper written by Hurr and Litke (1989) and published by the U.S. Geological Survey. It explains how groundwater withdrawals can be estimated using energy consumption data, i.e. how a conversion factor α can be computed. They suggest to use a multiple linear regression for explanatory variables being continuous rather than discrete, eventually yielding the best linear relation between the dependent variable and the explanatory ones. A short MATLAB script was written to conduct such an analysis. The model chosen was of the form:

$$\alpha = \beta_0 + \beta_1 x_1 + \beta_2 x_2 + \beta_3 x_3 + \beta_4 x_4 \tag{2.3}$$

β coefficients [-]
x_1 rated power of the pump [kW]
x_2 age of the pump [a]
x_3 depth to the static groundwater table [m]
x_4 friction factor λ of the piping in the well [-]

It contains the pump power since this value has a major impact on the Q-H relation. The age was introduced as the efficiency of a pump is expected to decrease with increasing age. The friction factor shall account for metal or plastic piping in the well and the associated friction losses. It was decided to build in the depth to the static water table rather than the dynamic one since more measurements thereof were available. The analysis was conducted for data from the second series of pumping tests as H was determined considerably more often during those. There was generally no pipe attached while they were carried out (as opposed to the first set). This is also the reason why the losses could not be featured explicitly in the above equation. To further minimise their effect on the results, the very few exceptions with piping of more than 6 m after the pump were excluded from this analysis.

2.3 Characteristic Curves Approach

A second approach involved the digitalisation of characteristic curves. From the Hebei Linquan Pump Co. Ltd., a data sheet could be obtained for a series of nationwide standardised pumps (QJ series). In 2011, a survey had been conducted in Guantao County regarding the characteristics of each well and pump. For all types featured in said data set (see table A.1 in the appendix), between six and eight data points for both the Q-H and Q-N_s relationship were read from the respective figure. These could then be stored in MATLAB variables which, in turn, served as a catalogue to retrieve information. Before polynomial curves could be fit to obtain curves such as the ones in figure 2.1, two more aspects had to be considered: First, pumps of the same type but different rated power feature a differing number of impellers. These so-called multistage pumps can supply greater heads while maintaining the same flow rate as their single-stage counterparts (Karassik et al., 2001). To calculate said number, the rated lift of the pump of interest is read from a table. This value is then simply divided by the respective value of a single-stage pump. The latter can be obtained from a characteristic curve plot and corresponds to the lift at the rated discharge. Multiplication of the discharge head and shaft power from e.g. figure 2.1 with the number of impellers leads to the respective values for a multistage pump. The second aspect is that N_s has to be divided by η_{motor} to calculate the required power to the motor N_m, as mentioned in section 2.1.1. Subsequently, polynomial curves of third (Q-H) and second order (Q-N_m) were fit to the data points. It was tried to keep their order generally low. The ones chosen reproduced the characteristic curves depicted in the data sheet most accurately. The Q-α relation can then simply be computed by dividing N_m by Q. An example of the two characteristic curves constructed is depicted in figure 2.2 for a 7.5 kW powered pump (blue and green line).

2.3.1 Experimental Data

To establish an experimental connection between electricity consumption and water volume pumped, two sets of pumping tests were conducted to date, both in Shoushansi District. The power was calculated based on readings of the electricity meter and counting time. The flow rate was determined by filling up a container of known volume and tracking the time and / or connecting a portable ultrasound flow meter to the piping. (Both methods to determine Q were found to deliver

similar results for a small sample of four wells.) During the first set carried out in March 2016, 101 wells were tested and characteristics such as the pump specifications as well as pipe diameter and estimated length recorded. The procedure was repeated in June cataloguing 581 wells and testing 104 thereof. 78 wells from the first field campaign were also part of the second one. As mentioned previously, the major difference between the two sets is that, in general, the distributional pipe was not attached to the pump during the second one. Due to the fact that some wells were tested in March and in June, one of the first tasks was to compare the records for age, power and rated lift of these. If discrepancies were found, the value of the second set was assigned as it was thought to be more reliable. However, the comparison also allowed to complete some information.
One issue with the results from the pumping testsa is that the meters installed by the State Grid Corporation of China turn faster so that the line losses are passed on to the end consumer. Representatives stated that 10 - 15 % are added in this way. However, it is not known whether the actual value is constant or varies throughout the region. Furthermore, the efficiency of a pump is expected to decrease with age due to wear of the parts. These two factors were assumed to cause the vertical spread in the data for pumps of the same rated power (cf. fig. 2.2). The horizontal spread was thought to be caused by differing pipe losses and types of pumps. The blue line represents an interpolation based on values read from the data sheet and would hence equal the performance of a new pump and an electricity meter turning at normal speed. It also functions as the lower bound for estimates of α. To obtain a mean value when the depth to the dynamic water table is given, this curve was stretched so it goes through the mean Q and mean α of the measurements (solid red line). The upper bound (dash-dot red line) was defined by stretching the characteristic curve to the highest measurements of the second set of pumping tests in order that all other values from the same set lie below. It would represent an old pump attached to a meter turning comparatively fast. Data from the second set was chosen to define the upper limit as no pipe was attached during the tests. This minimises the influence of pipe losses. Note that, nevertheless, some data points may be found below the lower bound, even if all curves digitalised for the respective power are printed. In parts, the uncertainty about the exact pump type is responsible. The second reason is that, even though these are standardised pumps, characteristic curves may vary from manufacturer to manufacturer. The Q-H curves were not adjusted since only a limited number of measurements of depth to the dynamic water table are available.

2.3.2 Historical Data

As mentioned at the beginning of the section, survey data is available from 2011 listing various things such as the locations of the wells, characteristics of the boreholes, pump specifications, the intended usage of the water, the irrigation area and an estimate of α. This list was reduced to 7028 wells in the shallow aquifer and 267 in the deep one, respectively, by excluding emergency backup wells plus the ones used to satisfy the domestic and industrial water demand. As shown in figure 1.2, measurements of the depth to static water table are available between 1973 and 2015. Since a drawdown could be observed over this period, pumps feasible for application now were not when water levels used to be higher. They would have been working inefficiently in the past. Therefore, the composition (or “mix”) of pumps must have changed and a computation of a

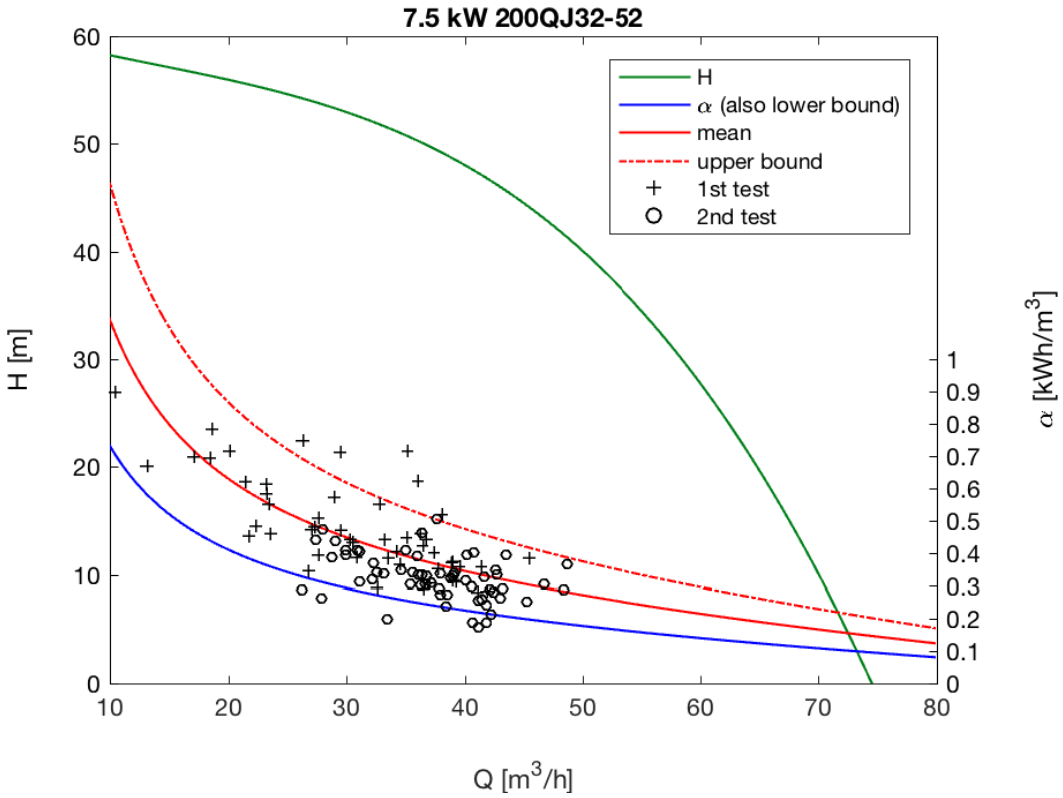

Figure 2.2: Polynomial curves describing the Q-H (green, left y-axis) and the Q-α relationship (blue, right y-axis) for a 7.5 kW pump with a rated discharge of 32 m^3/h and a rated lift of 52 m. The blue line also functions as the lower bound, whereas the mean curve (solid) and the upper bound (dash-dot) are depicted in red. The plus sign and the circles represent measurements of α from the first and second set of tests on wells featuring pumps of said power.

regional alpha should take this into account even if only a snapshot in time from 2011 is available. Information was obtained that farmers usually estimate the required lift by adding 20 - 30 m to the static water table depth. Hence the mean (25 m) was added to the available data (table A.2 in the appendix).

Shallow Aquifer

For wells penetrating the shallow aquifer, only twelve pumps feature a rated power in the range of 18.5 to 30 kW. The ones featuring 5.5 to 11 kW thus have been installed much more frequently. The two most common types in the second category are 175QJ32 and 200QJ32. It was assumed that no pumps with less than 4 kW had been installed since 1973 hence leading to a list of feasible ones presented in table 2.1. By far most farmers own a 7.5 kW pump according to the 2011 data (cf. column 4 in table 2.2). The development of the composition of the pumps, therefore, is expected to change from being 5.5 kW dominated (next lower power class available) to being 7.5 kW dominated when the measure used as the decision criterion (static depth plus 25 m) reaches the average of

Table 2.1: Feasible pump types for the shallow aquifer with a rated power between 4 and 11 kW and the mean rated lift of the two. There is no 200QJ32 pump available with a rated power of 9.2 kW. (Data: Hebei Linquan Pump Co. Ltd. (2015))

power [kW]	pump types	mean rated lift [m]
4	175QJ32-24 / 200QJ32-26	25
5.5	175QJ32-36 / 200QJ32-39	37.5
7.5	175QJ32-48 / 200QJ32-52	50
9.2	175QJ32-60	60
11	175QJ32-72 / 200QJ32-78	75

Table 2.2: Relative number of pumps of the corresponding power in the shallow aquifer in the "peak years". The values for 2011 were obtained from the survey data by excluding pumps featuring less than 7.5 and more than 11 kW. They were then transferred to the other years by shifting them by one pump power class.

	fraction [-]		
pump power [kW]	1973	1987.5	2011
4	0.881	0.000	-
5.5	0.112	0.881	0.000
7.5	0.007	0.112	0.881
9.2	0.000	0.007	0.112
11	-	0.000	0.007

the rated lifts of the two (43.75 m, cf. table 2.1). This occurred in 1996 as can be seen from the highlighted values in table A.2. The same procedure can be repeated for 4 and 5.5 kW (31.25 m), suggesting a change in 1979. It lead to the assumption that, in 1973, the 4 kW powered pumps were at their peak, halfway through 1987 (average of 1979 and 1996) the 5.5 kW took over and, eventually, in 2011 the 7.5 kW. From the survey data, the relative fraction of pumps with 7.5, 9.2 and 11 kW could be calculated and transferred to these other two "peak years" (table 2.2). 11 kW marks the upper limit of commonly installed pumps. Interpolating linearly between the years mentioned above allowed to define a pump mix for each year as shown in figure 2.3.

Deep Aquifer

The water level in the deep aquifer is considerably lower whereas the therefrom irrigated fields are generally larger, calling for pumps of higher rated power and discharge. The 18.5 to 30 kW ones are the most common while the prevalent two types are 200QJ63 and 250QJ80. Due to the fact that the water table used to be similarly high in both aquifers until 1978, it was assumed that, as in the shallow aquifer, 4 kW pumps had been employed in the beginning. It is thought that 5.5 kW powered ones (next higher power class available) followed on them. 7.5 kW pumps of the type

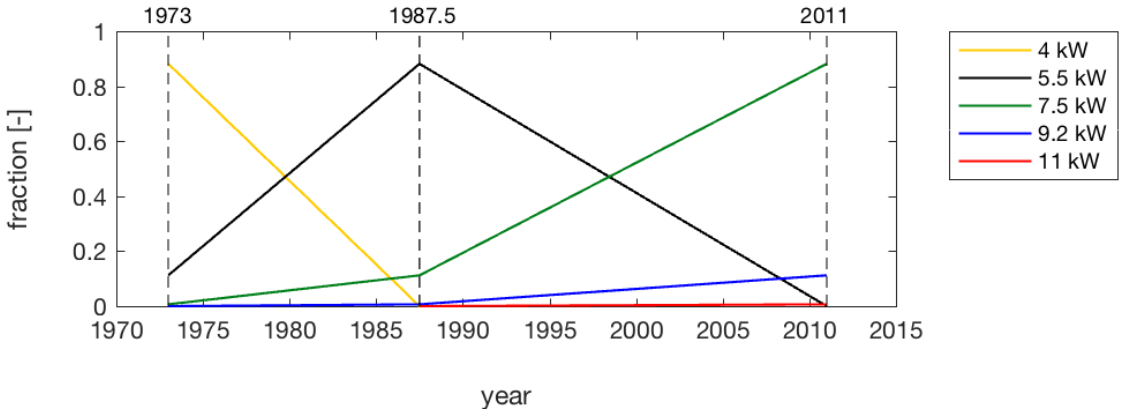

Figure 2.3: Evolution of the estimated relative composition of pumps exploiting the shallow aquifer between 1973 and 2010. The dashed lines mark years in which the mix was assumed to be known (1973 and 1987.5) or data is available (2011).

175QJ32-48 are the least powerful still in use in the deep aquifer, although installed only in four wells, and presumably represent the upper limit of low rated power motors. A list of feasible pumps could again be compiled (table 2.3). It was assumed that the two types from the shallow aquifer were common for 4 to 7.5 kW pumps. The procedure from above to assign the fractions could not be adopted one-to-one as the list is more extensive for this aquifer and covers a wider range. Most wells featured a 30 kW pump in 2011 (cf. column 6 in table 2.4). The second and third largest fraction consists of 18.5 and 22 kW pumps, respectively, although the difference is small. Since their mean rated lifts are of similar magnitude as well, they were treated as one class for this step with a mean rated lift of 63 m. The number of 25 kW powered ones was assumed to never having been dominant as they feature the second smallest fraction in the survey data and not the second largest as expected. The mean rated lift of two power classes was again averaged. By adding 25 m to the static water table data, years could be obtained where the dominant power was expected to having changed (highlighted values in table A.2), namely 1978 (4 → 5.5 kW, 31.25 m), 1986 (5.5 → 7.5 kW, 43.75 m), 1992 (7.5 → 18.5 / 22 kW, 56.5 m) and 2007 (18.5 / 22 → 30 kW, 75.5 m). (Note that the classification would not change if the above assumption regarding the 25 kW pumps never having been dominant would not hold. The dynamic water table reaches values above 84 m in 2012, although from 2011 onwards, the survey data was assumed to be representative.) The peak years were again defined to lie in between them (cf. table 2.4). Due to lack of information, it was assumed that during the first two periods (1973 - 1982 and 1982 - 1989), the number of pumps of lower power decreased at the same rate as the number of higher powered ones increased. The fractions for the year 2011 could be obtained from the survey data, as already mentioned. Halfway through 1999, fractions of 18.5 and 22 kW powered pumps were assumed to be rather high, as it is their peak year, and equal, since their mean rated lifts as well as their fractions in 2011 are of similar magnitude. 7.5 kW pumps were still found in the county in 2011 thus their fraction was set to 10 % in 1999.5. Pumps of the two highest power classes were expected to have started being introduced that very year. To calculate the pump composition between 1973 and 2010, the given

Table 2.3: Feasible pump types for the deep aquifer with a rated power between 4 and 30 kW and the mean rated lift of the two. There are no 250QJ80 pumps available with a rated power of 18.5 and 25 kW, respectively. (Data: Hebei Linquan Pump Co. Ltd. (2015))

power [kW]	pump types	mean rated lift [m]
4	175QJ32-24 / 200QJ32-26	25
5.5	175QJ32-36 / 200QJ32-39	37.5
7.5	175QJ32-48 / 200QJ32-52	50
18.5	200QJ63-60	60
22	200QJ63-72 / 250QJ80-60	66
25	200QJ63-84	84
30	200QJ63-96 / 250QJ80-80	88

Table 2.4: Relative number of pumps of the corresponding power in the deep aquifer in the "peak years". The values for 2011 were obtained from the survey data.

	fraction [-]				
pump power [kW]	1973	1982	1989	1999.5	2011
4	1.000	0.000	-	-	-
5.5	0.000	1.000	0.000	-	-
7.5	-	0.000	1.000	0.100	0.015
18.5	-	-	0.000	0.450	0.262
22	-	-	0.000	0.450	0.243
25	-	-	-	0.000	0.142
30	-	-	-	0.000	0.337

values were again interpolated linearly. Figure 2.4 shows the results. The nonlinear course of the lines for the four most powerful pumps arises from the fact that the code fails to find an α for 7.5 kW pumps at such low water levels. Hence it adjusts the fractions accordingly so that the sum is always equal to 1.

2.3.3 Computation of Regional α Values

To compute a regional value for $\alpha_{shallow}$ and α_{deep}, a code was written in MATLAB. It is split into two main parts. The first one computes a conversion factor for the years 1973 to 2010 (early period, EP), the second one for 2011 to 2015 (present period, PP). In a first step, the code compiles a list of feasible pump types based on the ranges in rated lift defined in tables 2.1 and 2.3 (EP) or observed in the 2011 survey data (PP). For the latter, it also performs minor adjustments regarding the pump power to standardise the entries. Figure 2.5 presents the further steps to compute an α_i for one individual well i in year t (PP) and for one pump power i in year t (EP), respectively. The depth to the dynamic water table H_{dyn} serves as the input (1). It is calculated by adding a constant value to the static one. If the year analysed falls into the present period (2), it searches

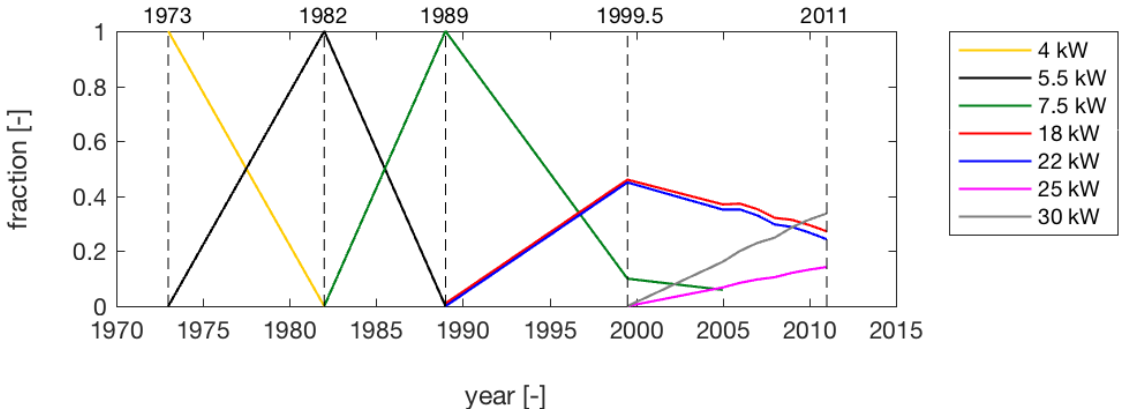

Figure 2.4: Evolution of the estimated relative composition of pumps exploiting the deep aquifer between 1973 and 2010. The dashed lines mark years in which the mix was assumed to be known (1973, 1982, 1989 and 1999.5) or data is available (2011).

for the pump with the closest rated Q and rated H (3) and, of course, equal power within the list mentioned above. For each pump type detected, the code finds a flow rate corresponding to H_{dyn} by solving for the polynomial root. These results are then restricted to values with an imaginary part equal to zero and which lie between 6 and 115 m^3/h. The range is given by the overall smallest and largest Q read from the data sheet when digitalising the characteristic curves. If no value met the criteria (4) and it was the first try (6), the code searches again for pumps in the list, although this time looking for the closest rated lift first and then rated discharge (3) (second try). If still no solution could be found, a "NaN" is assigned (6a). In the opposite case, the code calculates an α_i by inserting the respective Q into the polynomial function guarding the relationship. This will be the value assigned to the well if only one pump was closest (5b). If that was the case for multiple pumps, the arithmetic mean will be taken over (5a). The procedure is somewhat simpler for the years 1973 to 2010: For the respective aquifer, pump types listed in either table 2.1 (shallow) or 2.3 (deep) are selected (7). The α_i is eventually computed by multiplying the individual α_j with a factor f_j (7a). What lead to the introduction of f_j was the observation of a jump in the time series of the shallow conversion factor when transitioning from EP to PP, i.e. between 2010 and 2011. In this former version of the code, the formula in (7a) was the same as in (5a). Besides the difference in weighting explained in the next paragraph and the transition from interpolated to known composition of pumps, there is one more factor causing said jump. The two feasible pump types in the EP for e.g. a rated power of 5.5 kW may not be equally common while the arithmetic mean assumes this. Therefore, f_j simply expresses how often one type listed in tables 2.1 and 2.3 is chosen over the other one when the code computes $\alpha(2011)$ (e.g. 175QJ32 over 200QJ32). The respective values are presented in table 2.5 for both aquifers. 4 kW pumps were not present in the survey data. The α_j thus were averaged arithmetically which equals a weight of 0.5 here. The same applies to 5 kW for the deep aquifer. Even though four wells have a 7.5 kW pump installed there, it was chosen to weight them equally due to the small sample size. Pump powers with a "-"

Table 2.5: Factors f_j, sorted by relative diameter size D, for the shallow (columns 2 to 3) and deep aquifer (columns 4 to 5). They serve as weights to compute α_i between 1973 and 2010.

	$f_{j,shallow}$ [-]		$f_{j,deep}$ [-]	
pump power [kW]	small D	large D	small D	large D
4	0.50	0.50	0.50	0.50
5	0.15	0.85	0.50	0.50
7.5	0.73	0.27	0.50	0.50
9.2	1.00	0.00	-	-
11	1.00	0.00	-	-
18.5	-	-	1.00	0.00
22	-	-	0.16	0.84
25	-	-	1.00	0.00
30	-	-	0.17	0.83

were not featured in the respective aquifer between 1973 and 2010, a calculation was therefore not necessary or could not be carried out. For 9.2 (shallow) and 18.5 kW (deep), the factors had to be set to 1 and 0 as there is only one feasible type for those. Additionally, the code adjusts f_j if a solution can only be found for one pump type.
During the last step to obtain a final regional $\alpha(t)$, two different weighting approaches are applied, depending on the period the year of interest falls into. Since before 2011 there is no information available on neither the pump mix nor the irrigation area of each well, the factors from the linear interpolation of the pump composition in the county (figures 2.3 and 2.4) served as weights (e.g. $\alpha_{deep}(1976) = \frac{2}{3} \cdot \alpha_{i,deep,4kW}(1976) + \frac{1}{3} \cdot \alpha_{i,deep,5.5kW}(1976)$). However, this method calls for two assumptions: First, all wells supply fields of equal size with water and second, the water volume per unit area pumped is consistent throughout the county. While the latter has to hold for the years 2011 to 2015 as well, the former, i.e. the irrigated area, can be incorporated into the calculation of $\alpha(t)$. It provides the basis for the weighting factor β_i. The survey data was assumed to be representative for the whole PP. Although changes regarding this information have most certainly occurred on the pilot site since 2011, estimating a future pump mix and using weighting factors based on linear interpolation would presumably lead to higher uncertainties. Equation 1.1 can be formulated for well i and rearranged to:

$$\alpha_i = \frac{N_i}{Q_i} = \frac{N_i \cdot t_i}{Q_i \cdot t_i} = \frac{E_i}{V_i} \tag{2.4}$$

E_i electric energy consumption at well i [kWh]
V_i water volume pumped from well i [m^3]

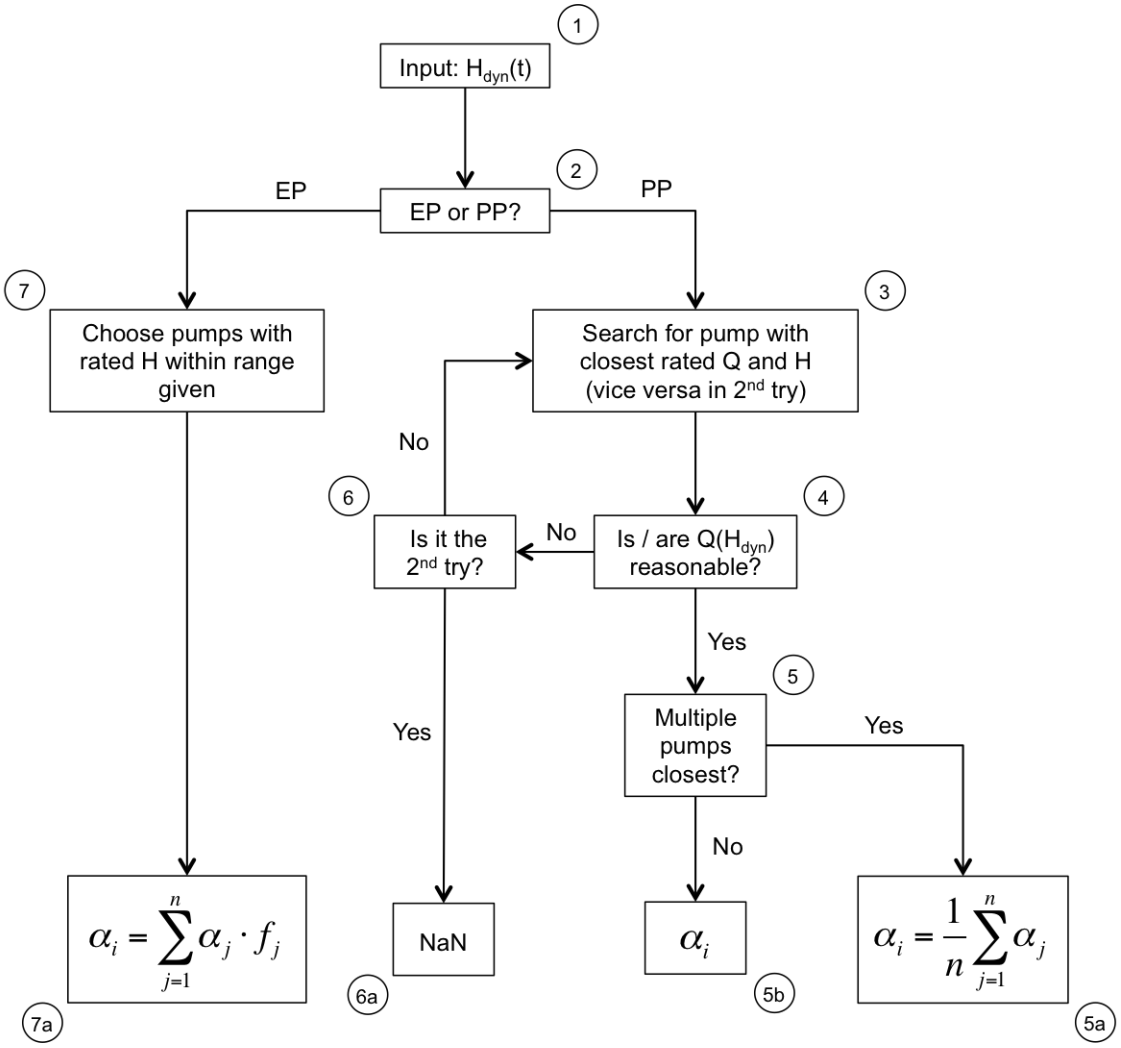

Figure 2.5: Flow chart explaining how the code computes an α_i depending on $H_{dyn}(t)$ for one individual well i (PP) and one class of pump power i (EP), respectively. EP stands for early period (1973 - 2010), PP for present period (2011 - 2015).

Table 2.6: Data which was used to stretch the Q-α characteristic curve, sorted by pump power and aquifer.

aquifer	pump power [kW]	data basis for stretch
shallow	4	mean stretch of 5.5 and 7.5 kW
	5.5 - 11	pumping tests
	18.5 - 30	survey data shallow aquifer
deep	4	as for the shallow aquifer
	5.5 - 7.5	pumping tests
	18.5 - 30	survey data deep aquifer

Under the assumption that q_i is constant, the individual α_i can be multiplied with β_i and summed up over all wells m to obtain a regional average:

$$\alpha = \frac{\sum_{i=1}^{m} E_i}{\sum_{i=1}^{m} V_i} = \frac{\sum_{i=1}^{m} V_i \cdot \alpha_i}{\sum_{i=1}^{m} V_i} = \frac{\sum_{i=1}^{m} A_i \cdot q_i \cdot \alpha_i}{\sum_{i=1}^{m} A_i \cdot q_i} = \frac{\sum_{i=1}^{m} A_i \cdot \alpha_i}{\sum_{i=1}^{m} A_i} = \sum_{i=1}^{m} \frac{A_i}{A_{tot}} \cdot \alpha_i = \sum_{i=1}^{m} \beta_i \cdot \alpha_i \tag{2.5}$$

A_i area irrigated by well i [mu] (1 mu $\widehat{=}$ 666.67 m^2)
A_{tot} total irrigated area in the county [mu]
q_i volume pumped per unit area [m^3/mu]
β_i irrigated area weighting factor [-]

As mentioned previously, the code uses the Q-H and then the Q-α relationship to compute a conversion factor based on the depth to the dynamic water table. During the second step, the stretch described in section 2.3.1 needs to be performed. The data providing the basis to do so varies with the aquifer and the pump power. A summary is shown in table 2.6. 4 kW pumps are not installed in the county hence no data is available. The stretch equals the mean stretch of the four pump types with 5 and 7.5 kW which were assumed to be feasible between 1973 and 2010. Since the types did not change for the deep aquifer, the data basis is the same. The survey data contains estimates of α as well. However, it seems that values were copied as many wells feature the exact same number. It is furthermore not exactly known how they were determined. Therefore, the pumping test data is believed to be more reliable for the range of 5 to 11 kW and was used for both aquifers. 13 kW is the highest power class tested thus the data basis for more powerful ones is provided by the survey data of the respective aquifer. The flow rate, however, is not listed in there. It was assumed to be equal to the rated Q of the pumps.

3 Results

3.1 USGS Method

Once a linear model has been fit, MATLAB displays a p-value for each coefficient. It corresponds to the hypothesis test of the respective coefficient β being equal to zero. If it lies below 0.05, the hypothesis can be rejected and the associated term is likely to be a meaningful addition to the model at the 5 % significance level. Additionally, the software contains a function to reduce the number of predictors (explanatory variables x) without changing the predictive accuracy (MathWorks Inc., 2016). Simplification of the model, however, lead to all coefficients besides β_0 and β_1 being set to zero. The pump power, therefore, has the highest influence. This is supported by the p-value of x_1 amounting to 0.008 and being considerably smaller than the ones for x_3 (0.062) and x_2 (0.192). It was decided to fit a second model but this time grouped by pump power. The term including the friction factor λ was also dropped as it featured the highest p-value (0.36). This resulted in a reduced equation of the form:

$$\alpha = \beta_0 + \beta_2 x_2 + \beta_3 x_3 \tag{3.1}$$

The availability of water table measurements mostly restricts the input data. Meaningful results could only be obtained for the 7.5 kW pumps since they featured a comparatively large sample size of 25 (out of a total of 39 for 5 pump power classes). Table 3.1 shows the computed β-values alongside their respective p-value. The constant term β_0 appears to have the largest effect on the computed α's followed by the age of the pump (x_2) and, eventually, the depth to the static water table (x_3). Figure 3.1 displays the computed versus the observed conversion factors using the results from table 3.1. The coefficient of determination between the two is very low and the spread is considerably larger vertically than horizontally.

Table 3.1: Coefficient values and the respective p-values for a linear regression model of the form $\alpha = \beta_0 + \beta_2 x_2 + \beta_3 x_3$ (equ. 3.1). Only data from wells featuring a 7.5 kW pump were taken into account.

coefficient	value [-]	p-value [-]
β_0	0.2661	0.052
β_2	0.0130	0.152
β_3	0.0011	0.817

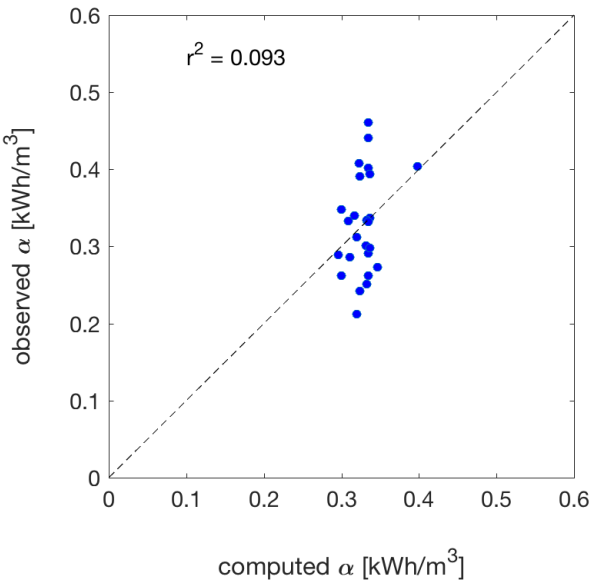

Figure 3.1: Computed α using the results from fitting a multiple linear regression (x-axis) versus observed values in the field (y-axis) for 7.5 kW powered pumps. Additionally, a straight line with a slope of 1 is mapped and the coefficient of determination indicated.

3.2 Characteristic Curves Approach

Figure 3.2 shows the computed time series of the regional α for the shallow and deep aquifer between 1973 and 2015. Moreover, it features the upper and lower bound as well as the dynamic depth to the water table. The estimated drawdown amounts to 7.35 m. This equals the average of a total of 38 measurements obtained during the two pumping tests in the shallow aquifer. Due to the unavailability of such data in the deep aquifer, the value was taken over. In both figures, the conversion factor increases with dropping water levels as more energy is consumed when a higher lift has to be provided. For the shallow aquifer, the slope is rather flat in the beginning but increases between 1987 and 2010. From 2011 onwards, where the survey data was assumed to be representative, it is close to zero. Here, the variations of 2.4 m in the water table convert to a change of only 0.0017 kWh/m^3 in α. Furthermore, the transition between EP and PP does not lead to a big jump (0.0085 kWh/m^3), as anticipated. A less smooth course of the curve would only be expected to occur due to a distinct and abrupt change in the water table or pump mix. The width between the upper and lower bound increases with time. Between 2011 and 2015, the upper bound is on average 26.5 % larger, the lower one 30.7 % smaller than the respective mean. For the deep aquifer, the increase of α over time starts out gentle as well and becomes faster after 1989. Starting from 2003, the at times erratic behaviour of the water level is reflected in the conversion factor. With the survey data as the basis between 2011 and 2015, the drop in the water table of 12.2 m shows up as an increase of 0.2332 kW/m^3 in α. The width between the upper and lower bound increases clearly over time. During the PP, the upper bound is on average 42.3 % larger,

the lower one 62.3 % smaller than the corresponding mean.
The results presented above can be combined if the total annual volume pumped from each aquifer is known. It would be very difficult to measure these quantities due to the large number of wells in the county. However, estimates could be obtained from the Handan Water Resources Public Report and the Department of Water Resources (DWR). $\alpha_{shallow}$ can be multiplied with the corresponding fraction of the total abstraction and added together with the respective value for the deep aquifer. The outcome of this analysis is shown in figure 3.3. Estimates from DWR regarding total volume pumped from the deep aquifer are available from 1994 until 2013, the data in the Handan Report covers the years 2004 to 2014. For the two sources, the therefrom calculated fractions are generally of similar magnitude. The highest differences exhibit the years 2004 and 2006 with a deviation of approx. 0.04. By the peaks occurring simultaneously with spikes in the coloured dash-dot lines, the influence of α_{deep} is clearly visible. The maximum variations to the curve for $\alpha_{shallow}$ from figure 3.2 amount to 0.074 kWh/m^3 in 2006 (Handan Report) and 0.065 kWh/m^3 in 2011 (DWR). The DWR data mentioned in the previous paragraph also represents an option to validate the calculated α. For the shallow aquifer, an estimate of the total electric energy consumed by irrigation E_{irr} is available. Based on equation 2.5, a relation between E_{irr} and $\alpha_{shallow}$ together with α_{deep} can be established (equ. 3.2) and rearranged to yield equation 3.3:

$$E_{irr} = V_{shallow} \cdot \alpha_{shallow} + V_{deep} \cdot \alpha_{deep} \tag{3.2}$$

$$V_{shallow} = \frac{E_{irr}}{\alpha_{shallow} + \frac{V_{deep}}{V_{shallow}} \cdot \alpha_{deep}} \tag{3.3}$$

Figure 3.4 depicts the DWR estimate of the volume pumped from the shallow aquifer versus the $V_{shallow}$ calculated based on electricity consumption. The red curve generally runs above the blue one. However, they show a similar course between 1997 and 2006. The mass balance error amounts to 43.9 %. Mostly the years from 2007 to 2014 feature large differences. Note as well that data for V_{deep} is only available from 1994 onwards. This may lead to an overestimate between 1991, when farmers started using deep groundwater for irrigation, and 1993 since the second term in the denominator in equation 3.3 becomes zero.
Furthermore, it was investigated how annual values of $\alpha_{shallow}$ compare to the ones representative for the irrigation seasons. Water level measurements of comparatively high temporal resolution provide the basis for said analysis. They were obtained from the Global Environment Facility (GEF) whose records encompass four years of data (2005 - 2008). The depth to the static water table in the shallow aquifer was measured every fifth day in the following three locations: in Shilidian and Nanyulin in the Weisengzhai District as well as in Beoidonggu in the Shoushansi District. The drawdown added was again assumed to be 7.35 m. For each data point, a mean regional conversion factor could then be computed (fig. 3.5). Contrary to expectations, a decrease in the water level leads to a decrease in $\alpha_{shallow}$ and vice versa. The dynamics in the water table, however, are clearly reproduced. In Shilidian, the overall mean conversion factor amounts to 0.3881 kWh/m^3.

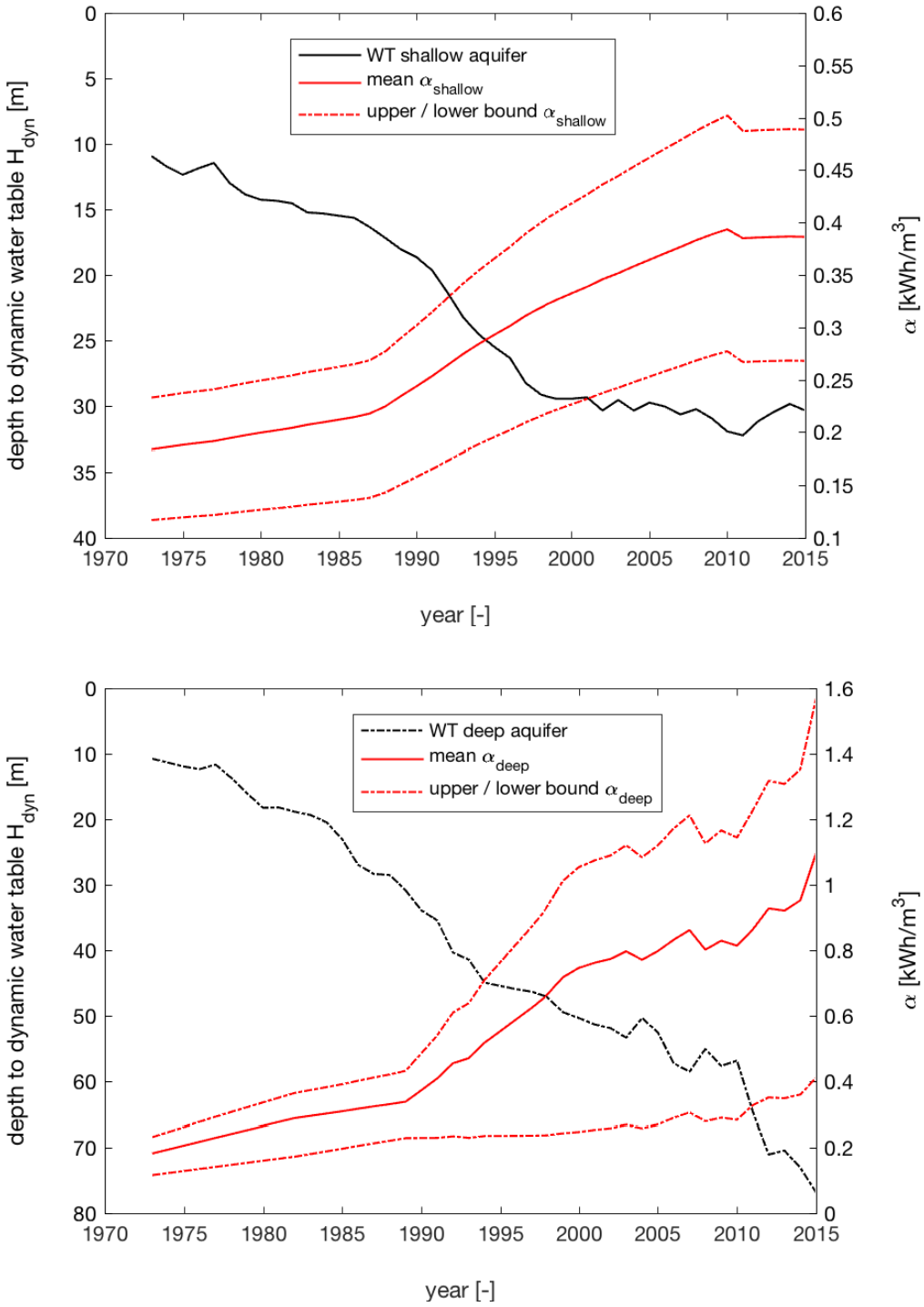

Figure 3.2: Estimates of the mean regional α (solid red) as well as its upper and lower bound (dash-dot red, right y-axis) between 1973 and 2015 for the shallow (top) and deep aquifer (bottom). The dynamic water level (solid and dash-dot black, respectively, left y-axis) was assumed to lie 7.35 m below the static one.

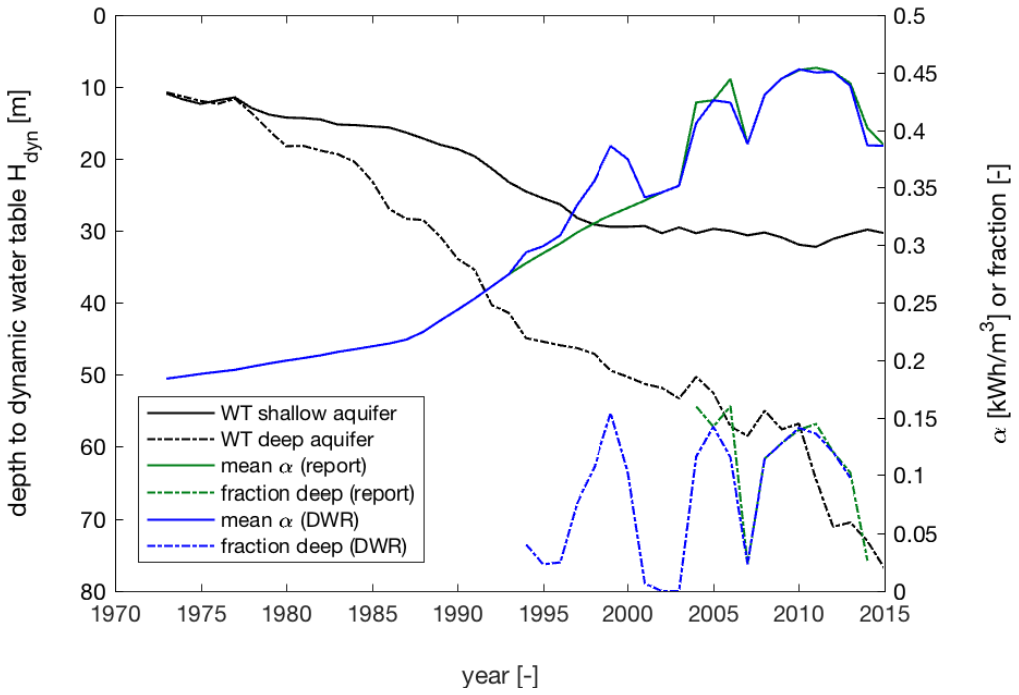

Figure 3.3: Time series of an α (right y-axis) representative of both aquifers between 1973 and 2015. Estimates of the volume pumped from each aquifer were obtained from the Handan Water Resources Public Report (green) and the Department of Water Resources (DWR, blue). The coloured dash-dot lines show the fraction from the deep aquifer (right y-axis). The dynamic water table in the two aquifers are again depicted as a solid and a dash-dot black line (left y-axis).

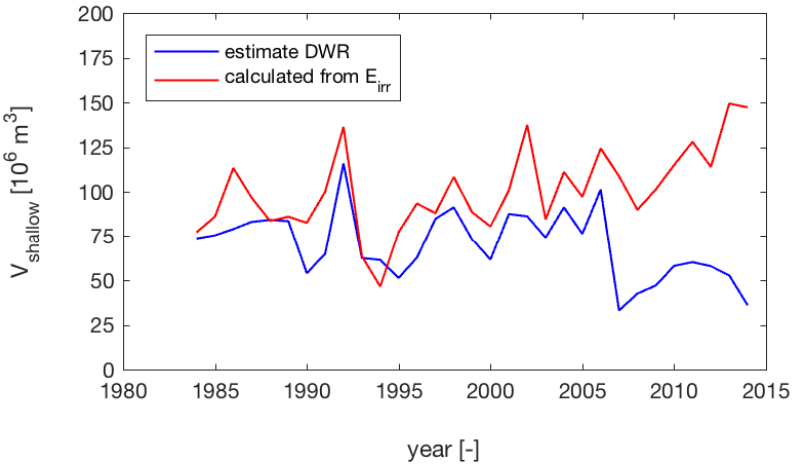

Figure 3.4: Total annual groundwater abstraction from the shallow aquifer (in Mm^3) as estimated by the DWR (blue) and as calculated based on energy consumption in combination with α (red) between 1984 and 2014.

The highest variation in the depth to the dynamic water table of 5.6 m converts to a change of 0.0049 kWh/m^3. In Nanyulin, the water table is highest on average, however, it also varies more. Here, the highest variation of 9.4 m causes a change of 0.0082 kWh/m^3. The mean $\alpha_{shallow}$ between 2005 and 2008 equals 0.3903 kWh/m^3. In Beidonggu, located in the same district as the wells tested by the ETH research team, the depth to the water table is highest on average. The overall mean conversion factor amounts to 0.3867 kWh/m^3. The highest variation in H_{dyn} of 4.8 m converts to a change of 0.0034 kWh/m^3. To compute mean values for the irrigation seasons, four such periods were defined:

- mid February - beginning of March (16.02. - 06.03)
- mid April - mid May (16.04. - 16.05.)
- mid June - beginning of July (16.06. - 06.07.)
- beginning of October - mid October (01.10. - 16.10.)

The start and end date of each period was set to days with measurements available. Table 3.2 lists an annual and the four periodical values for each GEF well location and for each year between 2005 and 2008. The periodical values are highest during the first irrigation season and generally lowest during the last one. However, minima may also occur during the second or third period. The maximum variations in periodical $\alpha_{shallow}$ at one location during one year are usually rather small. They amount to 0.0040 kWh/m^3 in Shilidian (2006), 0.0062 kWh/m^3 in Nanyulin (2005) and 0.0023 kWh/m^3 in Beidonggu (2006 and 2007), respectively. Consequently, differences between annual and periodical values are comparatively small as well and achieve maxima of 0.0026 kWh/m^3 in Shilidian (2006 and 2007), 0.0037 kWh/m^3 in Nanyulin (2005) and 0.0015 kWh/m^3 in Beidonggu (2007). The table can also be read vertically to compare values for the same period between locations. As expected, Beidonggu and Nanyulin, with the highest and lowest average water level, feature the largest differences. These reach values between 0.0047 kWh/m^3 and 0.0052 kWh/m^3. From 2005 to 2007, they occur during the first irrigation season; in 2008 during the fourth.
To perform a sensitivity analysis regarding the added drawdown, the calculations for the plots in figure 3.5 were repeated. Another 10 m were added to the 7.35 m to also come closer to the estimate of the farmers when they decide for a pump (static + 25...30 m). The results are depicted in figure 3.6. Here, $\alpha_{shallow}$ behaves as expected and decreases when the water table recovers. The dynamics in the depth to the water table are still reproduced. However, a threshold effect occurs as soon as H_{dyn} reaches values close to 40 m as can be seen from the distinct peaks. This also increased the overall mean conversion factor for Beidonggu by 0.9 % (to 0.3902 kWh/m^3) whereas it decreased for Shilidian by 0.7 % (to 0.3852 kWh/m^3) and for Nanyulin by 1.5 % (to 0.3844 kWh/m^3) compared to the data presented in figure 3.5.
Table 3.3 compiles again an annual as well as the four periodical values for the shallow conversion factor. It can be seen from the grey highlighted values that $\alpha_{shallow}$ increased nearly exclusively for the years 2006 to 2008: in Shilidian for the fourth irrigation season and in Beidonggu for the second, third and fourth one as well as for the annual means. The only exception in 2005 represents the second period in Nanyulin. For the annual mean conversion factors, relative changes between

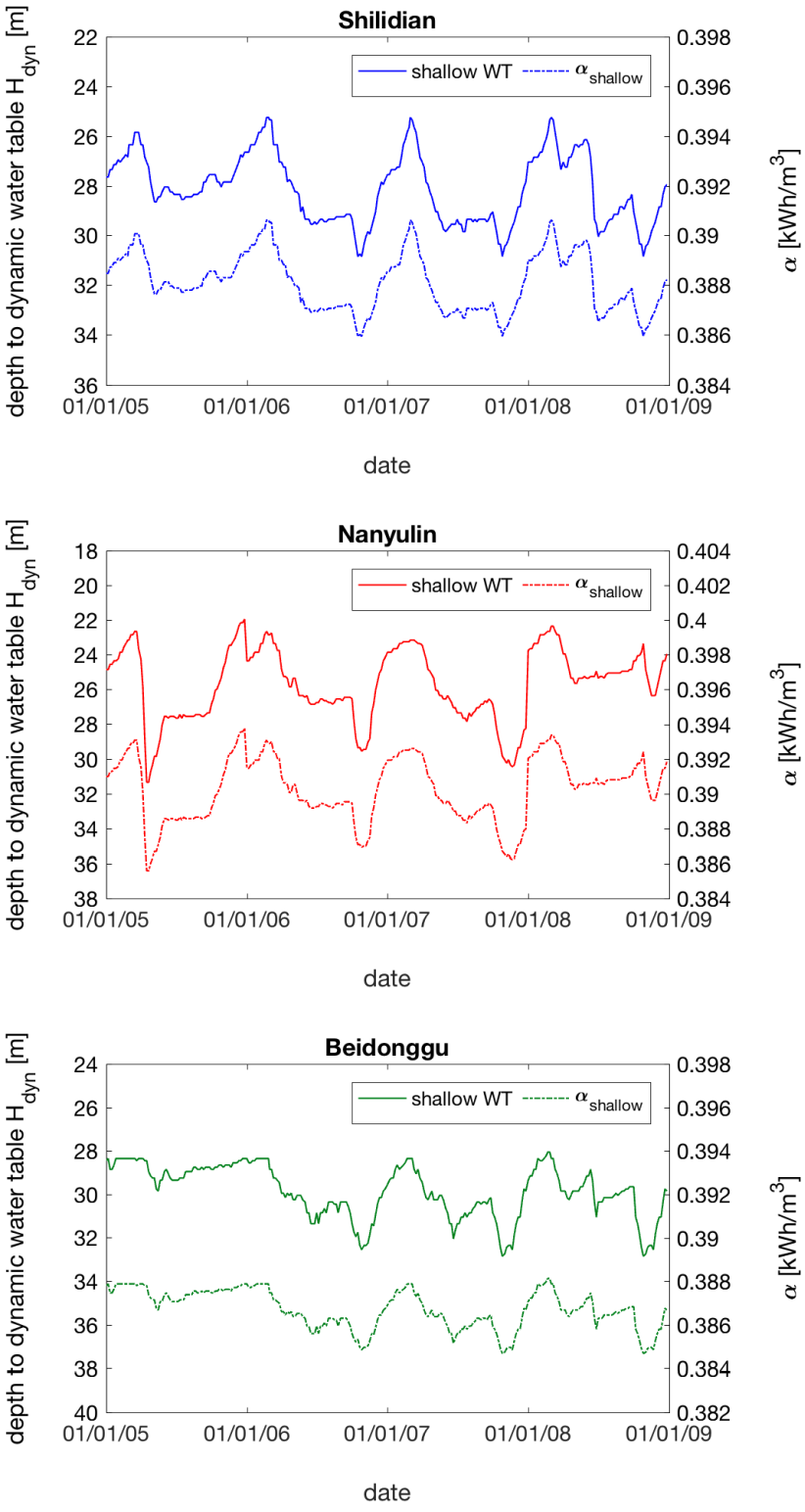

Figure 3.5: Water level measurements taken every fifth day (solid, left y-axis) in Shilidian (blue), Nanyulin (red) and Beidonggu (green) between 2005 and 2008. They served as an input to compute the respective $\alpha_{shallow}$ (dash-dot, right y-axis). The estimated drawdown equals 7.35 m.

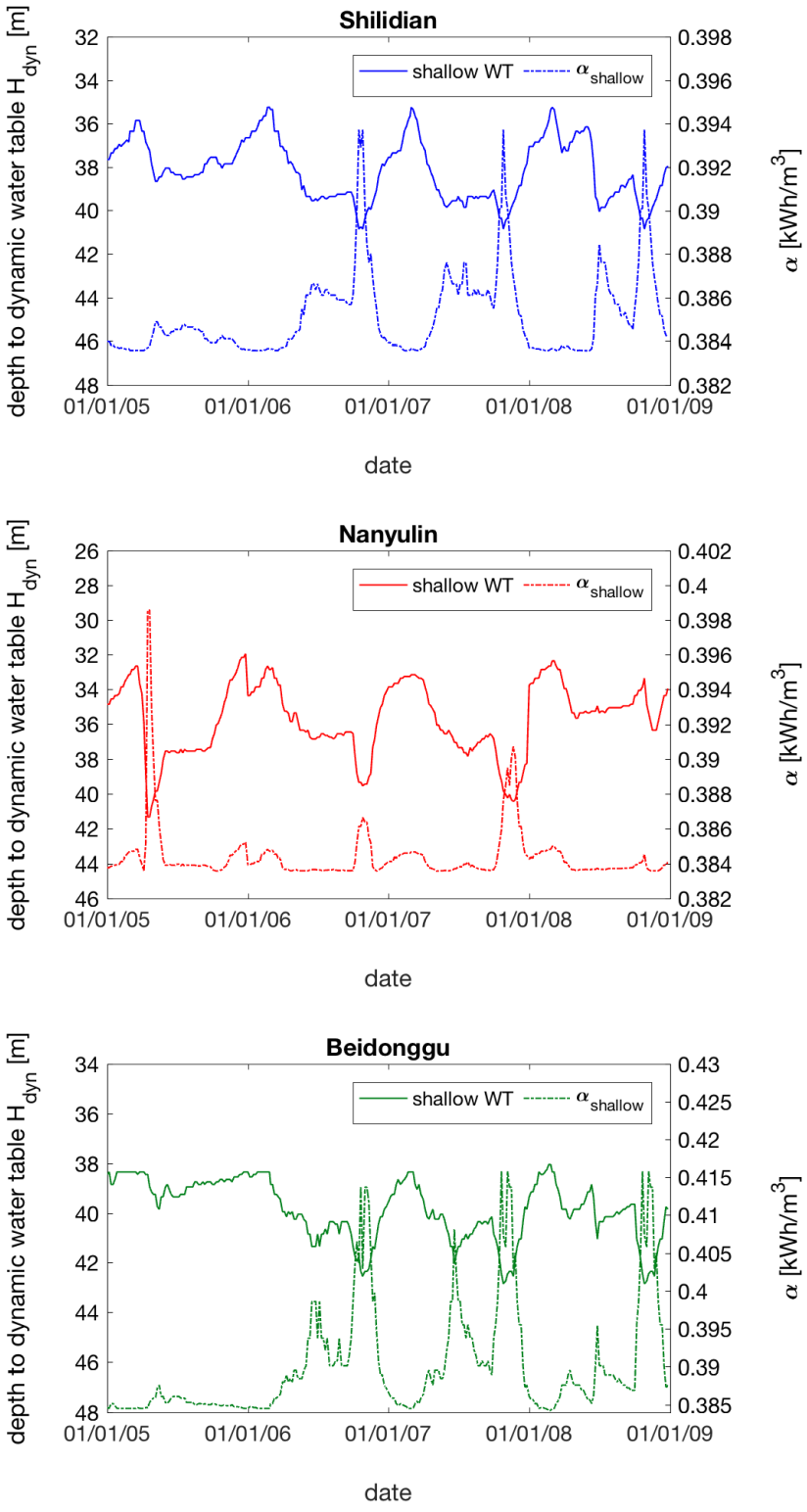

Figure 3.6: Water level measurements taken every fifth day (solid, left y-axis) in Shilidian (blue), Nanyulin (red) and Beidonggu (green) between 2005 and 2008. They served as an input to compute the respective $\alpha_{shallow}$ (dash-dot, right y-axis). The estimated drawdown equals 17.35 m.

Table 3.2: Mean annual as well as the four mean periodical $\alpha_{shallow}$ for the years 2005 to 2008 sorted by water level measuring location. The estimated drawdown equals 7.35 m.

	$\alpha_{shallow}$ [kWh/m^3]							
	2005		2006		2007		2008	
well location	annual	periodical	annual	periodical	annual	periodical	annual	periodical
Shilidian	0.3885	0.3894	0.3879	0.3905	0.3877	0.3903	0.3882	0.3903
		0.3882		0.3881		0.3876		0.3894
		0.3879		0.3869		0.3869		0.3871
		0.3885		0.3865		0.3868		0.3868
Nanyulin	0.3900	0.3925	0.3901	0.3929	0.3896	0.3925	0.3913	0.3932
		0.3863		0.3902		0.3904		0.3905
		0.3885		0.3892		0.3889		0.3907
		0.3896		0.3881		0.3883		0.3916
Beidonggu	0.3875	0.3879	0.3864	0.3877	0.3863	0.3878	0.3866	0.3880
		0.3872		0.3865		0.3865		0.3866
		0.3871		0.3857		0.3855		0.3864
		0.3875		0.3854		0.3856		0.3859

the same entries in the two tables are below 2 %. They range from 0.5 to 1.1 % in Shilidian, from 1.3 to 1.9 % in Nanyulin and from − 1.7 to + 0.6 % in Beidonggu. Among the periodical values, the relative differences are bigger although still below 5 %. They lie between − 0.7 and + 1.8 % in Shilidian, − 1.4 and + 2.1 % in Nanyulin and − 4.6 and + 0.9 % in Beidonggu.
One last investigation aimed at looking at the behaviour of $\alpha_{shallow}$ for one single pump. It was expected that effects may even out when computing a regional conversion factor. The data from Nanyulin was chosen as the input since it featured the highest variations and would most likely provide indications on this matter. A pump of the type 175QJ32-48 with a rated power of 7.5 kW served as the representative one since the code chooses it by the far most often when looking for the most suitable pumps (approx. 4'000 times). The drawdown was set to 7.35 m. Figure 3.7 shows the evolution of the water level and the conversion factor for the shallow aquifer over time. It stands out that the values are considerably elevated compared to their regional counterparts, namely 19.1 % or 0.0745 kWh/m^3 on average. Variations have increased as well and the maximum change in H_{dyn} of 9.4 m between April and December 2005 leads to a difference of 0.0285 kWh/m^3 in $\alpha_{shallow}$. Annual and periodical means can be found in table 3.4. The maximum variation between periodical $\alpha_{shallow}$ from the same year has increased and equals 0.0219 kWh/m^3 (2005). The largest difference between the annual and the periodical means is featured in 2005 as well and amounts to 0.0136 kWh/m^3. Relative changes compared to the data in table 3.2 are nearly equal to the ones observed in daily values (approx. 19.0 %). The results from figure 3.7 can also be used to determine time frames during which a pumping test should be performed so that the conversion factor obtained in the field is similar to the average one. Table 3.5 presents the periods or days during which this was the case when allowing for a deviation of ± 2.5%. There is no date listed in every year, however, the period from 1 May until 11 May is mentioned for 2006 to 2008.

Table 3.3: Mean annual as well as the four mean periodical $\alpha_{shallow}$ for the years 2005 to 2008 sorted by water level measuring location. The estimated drawdown equals 17.35 m. The grey highlighted values increased compared to the corresponding ones in table 3.2.

	$\alpha_{shallow}$ [kWh/m^3]							
	2005		2006		2007		2008	
well location	annual	periodical	annual	periodical	annual	periodical	annual	periodical
Shilidian	0.3841	0.3836	0.3856	0.3837	0.3858	0.3836	0.3853	0.3836
		0.3843		0.3843		0.3851		0.3836
		0.3845		0.3865		0.3865		0.3866
		0.3840		0.3894		0.3874		0.3874
Nanyulin	0.3849	0.3846	0.3841	0.3847	0.3847	0.3846	0.3840	0.3848
		0.3916		0.3836		0.3837		0.3837
		0.3839		0.3837		0.3837		0.3837
		0.3836		0.3847		0.3843		0.3840
Beidonggu	0.3851	0.3845	0.3921	0.3848	0.3929	0.3846	0.3906	0.3844
		0.3860		0.3886		0.3889		0.3879
		0.3861		0.3976		0.4012		0.3904
		0.3851		0.4031		0.3982		0.3965

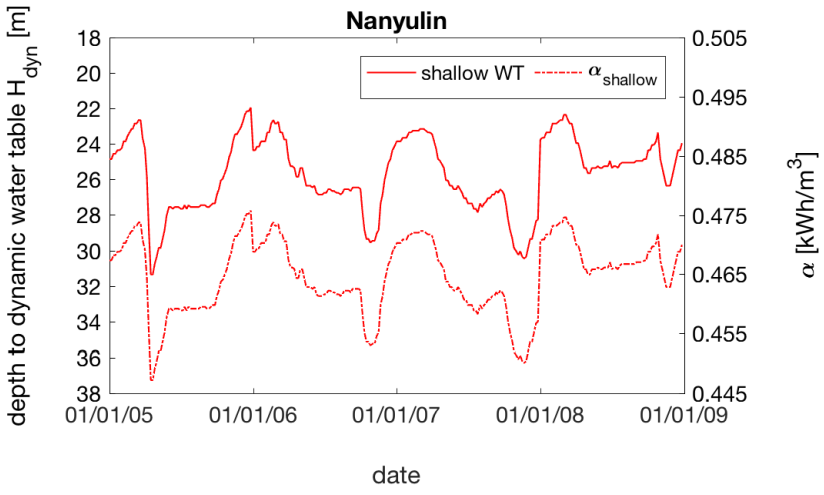

Figure 3.7: Water level measurements taken every fifth day (solid, left y-axis) in Nanyulin between 2005 and 2008. They served as an input to compute the respective $\alpha_{shallow}$ (dash-dot, right y-axis). The estimated drawdown equals 7.35 m.

Table 3.4: Mean annual as well as the four mean periodical $\alpha_{shallow}$ between 2005 and 2008 for a imaginary 175QJ32-48 pump located in Nanyulin. The estimated drawdown equals 7.35 m.

	$\alpha_{shallow}$ [kWh/m^3]							
	2005		2006		2007		2008	
well location	annual	periodical	annual	periodical	annual	periodical	annual	periodical
Nanyulin	0.4638	0.4721	0.4642	0.4733	0.4626	0.4721	0.4683	0.4740
		0.4502		0.4648		0.4653		0.4658
		0.4590		0.4614		0.4605		0.4662
		0.4628		0.4573		0.4582		0.4692

Table 3.5: Days or periods during which $\alpha_{shallow}$ was equal to its longterm mean (2005 to 2008) ± 2.5 %. The results are based on the data from Nanyulin.

2005	2006	2007	2008
06.04.	16.04. - 26.04.		21.04. + 26.04.
	01.05. - 11.05.	01.05. - 11.05.	01.05. - 21.05.
			01.06. + 06.06.
			01.07. + 16.07.
11.10. - 26.10.			
			06.11. + 11.11.
	01.12. + 06.12.		01.12. + 06.12.

4 Discussion and Conclusions

Two approaches were applied to compute a conversion factor on a regional scale taking influencing factors such as the pump type, its age and the depth to the water table into account. Annual averages could then be compared to periodical ones and, furthermore, to the corresponding values at a single location.

The linear model the first approach was based on was not able to reproduce the variations in the observed data accurately. As table 3.1 shows, the constant β_0 features the lowest p-value indicating that it is most likely to be a meaningful addition to the model. This becomes apparent in the rather narrow horizontal spread in figure 3.1. All data points get shifted by β_0 to the right but the influence of both age (x_2) and depth to the static water table (x_3) is too small to bring them closer to the dashed line. As a result of the visual interpretation and the very low coefficient of determination, these analyses were discontinued. However, the procedure should be kept in mind for similar studies as it is fairly simple and time-efficient, and the number of terms can easily be increased or decreased depending on the available data.

The subsequently chosen second approach was more specific. A critical point when computing the time series for the shallow and deep conversion factor (fig. 3.2), due to its influence on the shape of the curve, is the estimation of the pump mix. Since only one snap shot from 2011 was available, the therewith associated uncertainties are high. In an effort to minimise them as much as possible, the definition of the periods during which the dominant pumps work efficiently was based on how farmers estimate the required lift. The factor f_j (cf. fig 2.5) has an impact on the results as well. It weighs the α_j of the two feasible pump types from tables 2.1 and 2.3. The 2011 survey data is again the only reference point and it is likely that the ratio between e.g. 200QJ32 and 175QJ32 pumps varies over time. However, the introduction of f_j instead of averaging arithmetically considerably reduced the occurring jump in $\alpha_{shallow}$ from 2010 to 2011.

Comparison of the time series of $\alpha_{shallow}$ and α_{deep} shows that uncertainties in the latter are much bigger. The conversion factor for the deep aquifer is expected to be generally larger as more energy has to be spent to pump the same volume. However, the differences between the lower bounds of the two α's are considerably smaller compared to the mean curves and the upper bounds. This indicates that the stretching plays a central role. The two field campaigns did not aim at the deep aquifer and only pumps with a rated power between 5.5 and 13 kW were tested. Therefore, the basis for the stretch for α_{deep} for higher powered pumps is provided by the values found in the survey data (cf. table 2.6). It can clearly be seen how these influence the width between the upper and lower bound. The introduction of pumps with more than 7.5 kW was assumed to have started after 1989 (cf. fig. 2.4). At this point, the width starts to increase as the fraction of more powerful pumps rises. Until 1989, the band is much narrower where test data provided the basis for the stretch. The difference between the two conversion factors then leads to the spikes observed in

figure 3.3 when computing an α representative for both aquifers. The estimated fractions pumped from the deep aquifer do not go above 16 % thus the influence of α_{deep} was expected to be less apparent. Nevertheless, if data gained in the field would weaken the stretch for the deep conversion factor, the spikes would flatten to some extent.
Figure 3.4 shows that the total volume pumped from the shallow aquifer calculated based on electricity consumption is overestimated compared to values reported by the DWR. This translates to an underestimate of α. The differences are clearly higher between 2007 and 2014. There is no obvious reason for the systematic drop in the blue curve from 2006 to 2007 as the following years were not particularly wet. Neglecting them nearly halves the mass balance error from 43.9 % to 21.6 %. Especially between 1997 and 2006, the dynamics match up but there appears to be a general offset. Garduño and Foster (2010) indicate that the abstracted volume may be underestimated, however, they only make a statement about the year 2005. They report that $V_{shallow}$ for irrigation totalled 77.4 Mm^3 but actual withdrawals are thought to have reached 99.5 Mm^3. These values are very similar to the DWR estimate (76.4 Mm^3) and the estimate based on E_{irr} (97.2 Mm^3).
With water level measurements taken every fifth day, a time series of the shallow conversion factor with higher temporal resolution could be computed (fig. 3.5). By adding a drawdown of 7.35 m, the results were counter-intuitive as a dropping water table should lead to a increase in α. The reason therefor most likely lies in the characteristic curve of the most often installed pump type as determined by the code (175QJ32, fig. A.1). Its tail does nut run out smoothly (like the one in fig. 2.2) thus implying that for this type, increasing H may lead to a more efficient conversion factor. If another 10 m are added to the drawdown (fig. 3.6), α shows the intuitive behaviour. What may happen is that, as the drawdown is further increased, α for the 175QJ32 type decreases. The conversion factors of other types, however, are pushed further to the left where the Q-α relationship is stronger bent upwards leading to the spikes in figure 3.5. 7.35 m is anticipated to be a conservative estimate of the drawdown. Even though it equals the average measured during the two field campaigns, the dynamic depth to the water table could in some cases only be determined by lowering the dipper into the pipe. If water flows back into the borehole fast, the depth would be underestimated. Furthermore, continuous friction losses could not yet be included in the calculations due to lack in data. They would also be added on top of the drawdown, further increasing the difference to the static water level.
The comparisons made possible by tables 3.2 and 3.3 indicate that, on a regional scale, annual and periodical averages do not differ much among locations as well as among years. Therefore, an average conversion factor for either one year or one irrigation season determined at one location may be representative for the whole county. However, this does not hold on a local level (cf. table 3.4). The compared values vary by an average of approx. 19 %. Since one of the goals of the project is to be fair to the farmers, assigning an individual conversion factor to each well is important. Regional α may not be representative for every pump type. The data from figure 3.7 could also be used to determine during what time of the year a pumping test should be performed so that the result is close to the average (here between 2005 and 2008). Based on table 3.5, the beginning of May is suggested. An alternative, although less suitable, would be April.
Overall, the final methodology is rather specific compared to the USGS approach and involves more preparatory work. However, it also provides a framework which can be extended and adjusted.

The code could also be applied to a smaller spatial scale to determine e.g. a conversion factor for one transformer. Further development aims at incorporating continuous losses and improving the results, primarily by enhancing the data basis. The work on this thesis showed how important reliable records are and that they may help to reduce the influence of factors which cannot be controlled.

Bibliography

Al-Shemmeri, T. (2012). *Engineering Fluid Mechanics*. Bookboon.

Bollrich, G. (2013). *Technische Hydromechanik 1: Grundlagen*. 7th ed. Beuth.

Foster, S. and H. Garduño (2004). "China: Towards sustainable groundwater resource use for irrigated agriculture on the North China Plain". In: *Sustainable Groundwater Management, Lessons from Practice, Case Profile Collection* 8.

Garduño, H. and S. Foster (2010). "Sustainable groundwater irrigation approaches to reconciling demand with resources". In: *GW-MATE Strategic Overview Series* 4.

Gujer, W. (2007). *Siedlungswasserwirtschaft*. 3rd ed. Springer Berlin Heidelberg.

Hebei Linquan Pump Co. Ltd. (2015). *QJ QJR QJB Series: Submersible Pumps Data Sheet*.

Hurr, R. T. and D. W. Litke (1989). *Estimating pumping time and ground-water withdrawals using energy-consumption data*. U.S. Geological Survey Water-Resources Investigations Report 89-4107.

Jia, Y. (2011). "Groundwater issues and management in the North China Plain". In: *Groundwater Management Practices*. CRC Press, pp. 45–56.

Karassik, I. J., J. P. Messina, C. C. Heald and P. Cooper (2001). *Pump Handbook*. 3rd ed. McGraw-Hill.

Liu, C., J. Yu and E. Kendy (2001). "Groundwater Exploitation and Its Impact on the Environment in the North China Plain". In: *Water International* 26.2, pp. 265–272.

MathWorks Inc. (2016). *MATLAB 2016b Documentation*.

Sultanian, B. (2015). *Fluid Mechanics: An Intermediate Approach*. CRC Press.

Xu, Y., S. Li and Y. Cai (2005). "Wavelet analysis of rainfall variation in the Hebei Plain". In: *Science in China Series D: Earth Sciences* 48.12, pp. 2241–2250.

Appendix

The Haaland equation (Sultanian (2015)) was used for an initial guess of the friction factor λ:

$$\frac{1}{\sqrt{\lambda}} = -1.8 \cdot \log_{10}\left(\frac{6.9}{Re} + \left(\frac{k/D}{3.7}\right)^{1.11}\right) \tag{A.1}$$

The dimensionless Reynolds number in a circular pipe is calculated as follows (Gujer, 2007):

$$Re = \frac{v \cdot D}{\nu} \tag{A.2}$$

Equation A.2 requires the kinematic viscosity ν as an input. It has the units of [m^2/s] and equals, on the other hand, η/ρ. The density of water was set to 1000 kg/m^3 whereas the dynamic viscosity η can be estimated with the formula (Al-Shemmeri, 2012):

$$\eta = 2.414 \times 10^{-5} \cdot 10^{247.8/(T-140K)} \tag{A.3}$$

η dynamic viscosity [kg/(m · s)]
T temperature of the water [K]

The groundwater temperature was only measured on roughly 2/3 of the wells during the first set of pumping tests. If available, measurements were used to calculate η. If T had not been measured or for analyses regarding the second series of pumping tests, the mean value of 16.36 °C served as in input.

Table A.1: Pump types (manufacturer: Hebei Linquan Pump Co. Ltd.), for which the characteristic curves were digitalised, sorted by pipe diameter. The QJ series is a range of submersible pumps following a national standard.

175 mm	200 mm	250 mm
	200QJ25	
175QJ32	200QJ32	
175QJ40	200QJ40	250QJ40
175QJ50	200QJ50	250QJ50
	200QJ63	250QJ63
	200QJ80	250QJ80

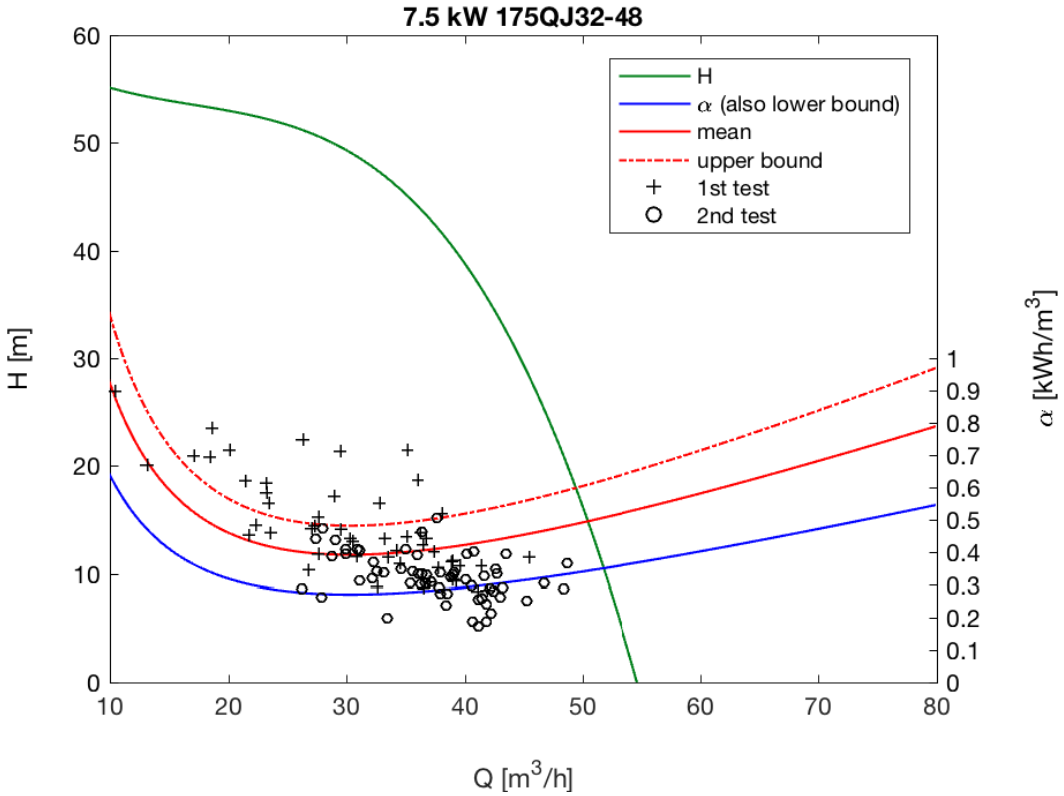

Figure A.1: Q-H (green, left y-axis) and Q-α relationship (blue, right y-axis) for a pump of the type 175QJ32-48 with a power of 7.5 kW. The plus signs and circles represent measurements of the conversion factor from the corresponding set of pumping tests.

Table A.2: Mean depth to the static water table in the shallow and deep aquifer in Guantao County between 1973 and 2015 obtained by averaging a measurement from May and September. The dynamic one listed here was calculated by adding 25 m and was afterwards used to assume a pump mix in the area. The grey highlighted values mark years where the dominating pump power is thought to have changed.

	depth to shallow water table		depth to deep water table	
year	static [m]	dynamic [m]	static [m]	dynamic [m]
1973	3.58	28.58	3.41	28.41
1974	4.40	29.40	4.00	29.00
1975	5.00	30.00	4.60	29.60
1976	4.52	29.52	5.00	30.00
1977	4.10	29.10	4.30	29.30
1978	5.62	30.62	6.35	31.35
1979	6.50	31.50	8.73	33.73
1980	6.91	31.91	10.90	35.90
1981	6.99	31.99	10.85	35.85
1982	7.18	32.18	11.50	36.50
1983	7.88	32.88	12.00	37.00
1984	7.96	32.96	13.10	38.10
1985	8.13	33.13	15.70	40.70
1986	8.29	33.29	19.60	44.60
1987	9.00	34.00	21.00	46.00
1988	9.83	34.83	21.16	46.16
1989	10.70	35.70	23.50	48.50
1990	11.30	36.30	26.55	51.55
1991	12.30	37.30	28.10	53.10
1992	14.02	39.02	33.00	58.00
1993	15.90	40.90	34.10	59.10
1994	17.20	42.20	37.60	62.60
1995	18.15	43.15	38.10	63.10
1996	19.00	44.00	38.60	63.60
1997	20.90	45.90	39.00	64.00
1998	21.80	46.80	39.80	64.80
1999	22.10	47.10	42.10	67.10
2000	22.10	47.10	43.00	68.00
2001	22.00	47.00	43.98	68.98
2002	23.00	48.00	44.53	69.53
2003	22.17	47.17	45.95	70.95
2004	21.99	46.99	43.00	68.00
2005	22.43	47.43	45.23	70.23
2006	22.69	47.69	49.95	74.95
2007	23.26	48.26	51.20	76.20
2008	22.92	47.92	47.66	72.66
2009	23.60	48.60	50.31	75.31
2010	24.56	49.56	49.48	74.48
2011	24.87	49.87	57.27	82.27
2012	23.83	48.83	63.68	88.68
2013	23.14	48.14	63.07	88.07
2014	22.46	47.46	65.70	90.70
2015	23.00	48.00	69.53	94.53